Stereoselective Effects of Monoterpenes on the Microviscosity and Curvature of Model Membranes Assessed by DPH Steady-State Fluorescence Anisotropy and Light Scattering Analysis

MARÍA P. ZUNINO,[1] ANAHI V. TURINA,[2] JULIO A. ZYGADLO,[1] AND MARÍA A. PERILLO[2]*

[1]*IMBIV-CONICET-ICTA, Cátedra de Química Orgánica, Facultad de Ciencias Exactas, Físicas y Naturales, Universidad Nacional de Córdoba, Córdoba, Argentina*

[2]*Biofísica-Química, Cátedra de Química Biológica, Depto. de Química/ICTA, Facultad de Ciencias Exactas, Físicas y Naturales, Universidad Nacional de Córdoba, Córdoba, Argentina*

ABSTRACT Here, we evaluated stereoselectivity in monoterpenes (MTs) ability to disturb membrane dynamics. Correlations between molecular structure and physicochemical properties of pinenes, menthols, and carvones enantiomers were investigated through cluster and principal component analysis. Therefore, MTs' concentration-dependent changes in light scattering and diphenylhexatriene (DPH) fluorescence polarization induced by MTs were measured on large unilamellar vesicles (LUVs) of dipalmitoylphosphatidylcholine. The behavior of the less polar compounds (hydrocarbons) was characterized by a membrane expansion (increase in light scattering), detectable within the low-concentration range. They remained in the membrane up to the highest concentrations tested exhibiting a concentration-dependent anisotropy decrease. Within the more polar terpenes (alcohols) prevailed a budding phenomenon with the production of small LUVs with roughly constant curvature (more evident at medium and high concentrations), which explains the slight change in microviscosity (DPH fluorescence anisotropy). These behaviors were compatible with the deeper localization within the membrane core of the formers compared with the latters as predicted from the corresponding polar charge distribution in their molecular structures. The enantioselectivity was expressed by neomenthol at low concentration and carvone at medium concentration. Inhibition and potentiation were evidenced, within the low-concentration range, by the racemic mixtures in neomenthol and β-pinenes, respectively. *Chirality 23:867–877, 2011.*

KEY WORDS: terpenes; stereoisomers; racemic mixtures; DPH fluorescence anisotropy; membrane organization; membrane disruption

INTRODUCTION

Terpenes are plant-based organic compounds formed by isoprene units. They are the major components of plant "essential oils." Terpenes are usually synthesized by plants in response to stress conditions and they result effective against infectious or parasitic agents.[1] These natural products are also used as raw materials in many fields, including perfumes, cosmetics, aromatherapy and phytotherapy, spices, and nutrition. Although numerous reports have been published on the bioactivity of essential oils and pure terpenes,[2] knowledge of the mode of action is limited.[3] Among them, antimicrobial activity induced by a great number of terpenes has been studied and correlated with their molecular properties and lipophilic characteristics.[4,5] In addition, monoterpenes (MTs) are known to affect sterol and fatty acid composition in plants.[6,7]

Lipophilic compounds such as MTs can be accumulated at varying depths in the membrane bilayer depending on their hydrophobicity and the presence of functional groups such as hydroxyl-, carboxyl-, or phenyl groups in their molecular structure. Depending on their location at the membrane, intermolecular interactions within either the head group or the acyl chains region may be disturbed[8–10] and membrane function may be affected.[11–15]

Many terpenes contain one or more asymmetric carbon atoms that exhibit optical activity. These chiral compounds of natural origin (monoterpenes and sesquiterpenes) are generally found in characteristic enantiomeric distributions because they have evolved via enzymatically controlled biosynthetic pathways.[16] Enantiomeners may exhibit differential properties. This may be ascribed to the stereoselectivity of the binding mechanism of bioactive chemicals with biological receptors. This enantioselectivity has been studied in the insect communication systems,[17,18] in the absorption rate of an enantiomeric pair of fragrance compounds,[19] and in the activity of $GABA_A$ receptor[3,20] among others. Each stereoisomer contributes to the beneficial or adverse effects of these compounds. Moreover, synergistic and antagonistic actions

Abbreviations: $\%\Delta A$, anisotropy change percent; $\%\Delta LI_{356}$, light intensity at 356-nm change percent; (−)-AP, (−) α-pinene; (+)-AP, (+) α-pinene; (−)-BP, (−) β-pinene; (+)-BP, (+) β-pinene; (−)-C, (−) carvone; (+)-C, (+) carvone; DPH, diphenylhexatriene; dpPC, dipalmitoylphosphatidylcholine; FI, fluorescence intensity; Gr., group; (+)-IM, (+) isomenthol; LUVs, large unilamellar vesicles; (−)-M, (−) menthol; (+)-M, (+) menthol; MLVs, multilamellar vesicles; MT, monoterpene; (−)-NM, (−) neomenthol; (+)-NM, (+) neomenthol; $P_{o/w}$, octanol/water partition coefficient; PCA, principal component analysis; VDW, van der Waals area for solvation.

Contract grant sponsors: CONICET, SECyT-Universidad Nacional de Córdoba, Mincyt-Provincia de Córdoba, and ANPCyT from Argentina.

*Correspondence to: María Angélica Perillo, Facultad de Ciencias Exactas, Físicas y Naturales, Universidad Nacional de Córdoba, Av. Vélez Sarsfield 1611, X5016GCA Córdoba, Argentina. E-mail: mperillo@efn.uncor.edu

Received for publication 7 July 2010; Accepted 19 May 2011
DOI: 10.1002/chir.20998
Published online 20 September 2011 in Wiley Online Library (wileyonlinelibrary.com).

are observed with MTs and their enantiomers in bacteria, seedlings, and insects.[2,21]

The understanding of the action mechanism of drugs, including MTs, at a molecular level is simplified with the use of model membranes such as liposomes,[22] which allow sensing and hopefully interpreting the origin of subtle changes in particular membrane properties upon drug binding and can also be used as a screening tool. Up to our knowledge, differential behavior of enantiomers in model membranes has not been investigated. This is important because it is often overlooked that enantioselectivity in the activity of enantiomers as determined in vitro cannot be extrapolated to the in vivo situation because enantioselective drug disposition can lead to an enantiomer ratio in vivo, which differs substantially from that in the dosage form administered.[23] Enantioselectivity in drug disposition seems to be the rule rather than the exception, and depending on whether the active or less active enantiomer is preferentially affected, there may be amplifications of attenuations in drug potency in vivo when compared with that observed in vitro.[24] In addition, to extrapolate the predictions derived from analysis in vitro, another factor that should be taken into account is drug effect on the molecular environment. One may feel tempt to think that action mechanisms exerted through the drug binding to recognition sites in receptor proteins would assure a particular specific effect. However, in view of the dynamic organization of membrane, stereospecificity becomes a relative concept because of the coupling between conformation of protein receptors and the organizational dynamics of their molecular surroundings in the membrane.[25,26] The relevance of the stereochemistry in defining partitioning, location, penetration, and permeability of MTs across membranes may help understanding how disposition and effects on the molecular environment modulates final estereoselectivity of MTs observed in in vivo.

Previous work on model membranes showed that several MTs penetrated in monomolecular layers of dipalmitoylphosphatidylcholine (dpPC) at the air–water interface, even at surface pressures above the equilibrium lateral pressure of bilayers. They affected the self-aggregation of Triton X-100, increasing its critic micellar concentration, and increased the surface curvature of soybean phosphatidylcholine vesicles, suggesting their location at the polar head group region of the membrane.[10] The latter was supported by their ability to increase differentially the polarity of the membrane environment sensed by two electrochromic dyes.[9] The location of MTs at the polar head group region of membranes precludes their ability to increase the surface curvature upon their incorporation in bilayers. In vesicles, this phenomenon may lead to a decrease in particle diameter[27] and could be assessed by a decrease in the scattering of light.

Fluorescence anisotropy is a widely applied technique to estimate microviscosity and/or molecular organization of bilayer model membranes, and diphenylhexatriene (DPH) is often the probe of choice for this kind of studies.[28–31] DPH is an environmentally sensitive fluorescent probe known to be located within the hydrocarbon chain region of the membrane core,[32] exhibits a strong fluorescence increase upon binding to lipids, and has sensitive polarization (anisotropy) responses to phospholipid orientational order.

This article was aimed at trying to disclose a stereoselectivity in the ability of MTs to disturb the membrane dynamics and the extent at which this could be correlated with the expression of the bioactivities of these natural products. Hence, possible correlations between the structure and molecular properties of the enantiomers within three groups of MTs (pinenes, menthols, and carvones) were investigated by monitoring changes in light scattering and in the fluorescence polarization of DPH induced by MTs on large unilamellar vesicles (LUVs) of dpPC. The results were interpreted in terms of changes in membrane curvature, order, and dynamics.

MATERIALS AND METHODS

Materials

All reagents and solvents used were of analytical grade. Monoterpenes (MTs): (1*R*,2*S*,5*R*)(−)-5-methyl-2-(1-methylethyl)-cyclohexanol [(−)-menthol]; (1*S*,2*R*,5*S*)(+)-5-methyl-2-(1-methylethyl)-cyclohexanol [(+)-menthol]; (1*S*,2*R*,5*R*)(+)-5-methyl-2-(1-methylethyl)-cyclohexanol [(+)-isomenthol]; (1*S*,2*S*,5*R*)(+)-5-methyl-2-(1-methylethyl)-cyclohexanol [(+)-neomenthol]; and (1*R*,2*R*,5*S*)(−)-5-methyl-2-(1-methylethyl)-cyclohexanol [(−)-neomenthol]; (1*S*,5*S*)-6,6-dimethyl-2-methyli denebicyclo[3.1.1]heptane [(−)-β-pinene]; (1*R*,5*R*)-6,6-dimethyl-2-methylidenebicyclo[3.1.1]heptane [(+)-β-pinene]; (1*S*,5*S*)-4,7,7-trimethylbicyclo[3.1.1]hept-3-ene [(−)-α-pinene]; (1*R*,5*R*)-4,7,7-trimethylbicyclo [3.1.1]hept-3-ene [(+)-α-pinene]; (5*R*)-2-methyl-5-(prop-1-en-2-yl)cyclohex-2-enone [R-carvone]; and (5*S*)-2-methyl-5-(prop-1-en-2-yl)cyclohex-2-enone [S-carvone] were obtained from ICN Pharmaceuticals (Costa Mesa, CA), Aldrich Chemical company, or Fluka Chemicals; DPH from Sigma-Aldrich Chem (St. Louis, MO), and lipids (dipalmitoylphosphatidylcholine, dpPC) were purchased from Avanti Polar Lipids (Alabaster, Alabama) and were used without further purification.

Preparation of Large Unilamellar Vesicles

MLVs were prepared as described elsewhere.[33] The appropriate amount of dpPC dissolved in chloroform was placed in a glass tube and evaporated under a stream of nitrogen with constant rotation of a test tube so as to deposit a uniform film over the bottom third of a tube; traces of solvent were removed under vacuum. The dried lipid was suspended in water at a final concentration of 41 μM (0.03 mg/ml) by repeating seven consecutive cycles of heating at 65°C for 1 min plus vortexing for 30 sec, and MLVs were formed. LUVs were obtained by extruding 19 times the MLVs suspension trough 100-nm pore size Whatman polycarbonate filters using a miniextruder Liposofast (Avestin, Canada).

Steady-State Fluorescence

The fluorescent probe DPH (4 μM) was added to the dpPC LUV suspension (prepared as described above) and incubated for 1 h at room temperature. The effect of MTs (0–2 mM) on DPH steady-state fluorescence anisotropy was studied. Anisotropy values were calculated from the emission fluorescence intensities at λ_{em} = 430 nm (λ_{ex} = 356 nm) measured with the excitation, and the sample polarizer filters oriented parallel and perpendicularly one with respect to the other, in a L-format FluoroMax-3 spectrofluorometer (Jovin Yvon, Horiba). Slits width and integration time were set at 2 nm and 1 sec, respectively.

Because of their low water solubility, stock solutions of MTs were prepared in ethanol. The final ethanol concentration did not exceed 1.5% v/v. Control samples containing ethanol were tested to rule out the effect of this solvent.

Steady-state fluorescence anisotropy (A) was calculated as follows:

$$A = \frac{I_{VV} - I_{VH}.G}{I_{VV} + 2.I_{VH}.G} \qquad G = \frac{I_{HV}}{I_{HH}},$$

where I_{VV}, I_{HH}, I_{VH}, and I_{HV} are the values of the different measurements of fluorescence intensity taken with both polarizers in vertical (VV) and horizontal (HH) orientations or with the excitation polarizer

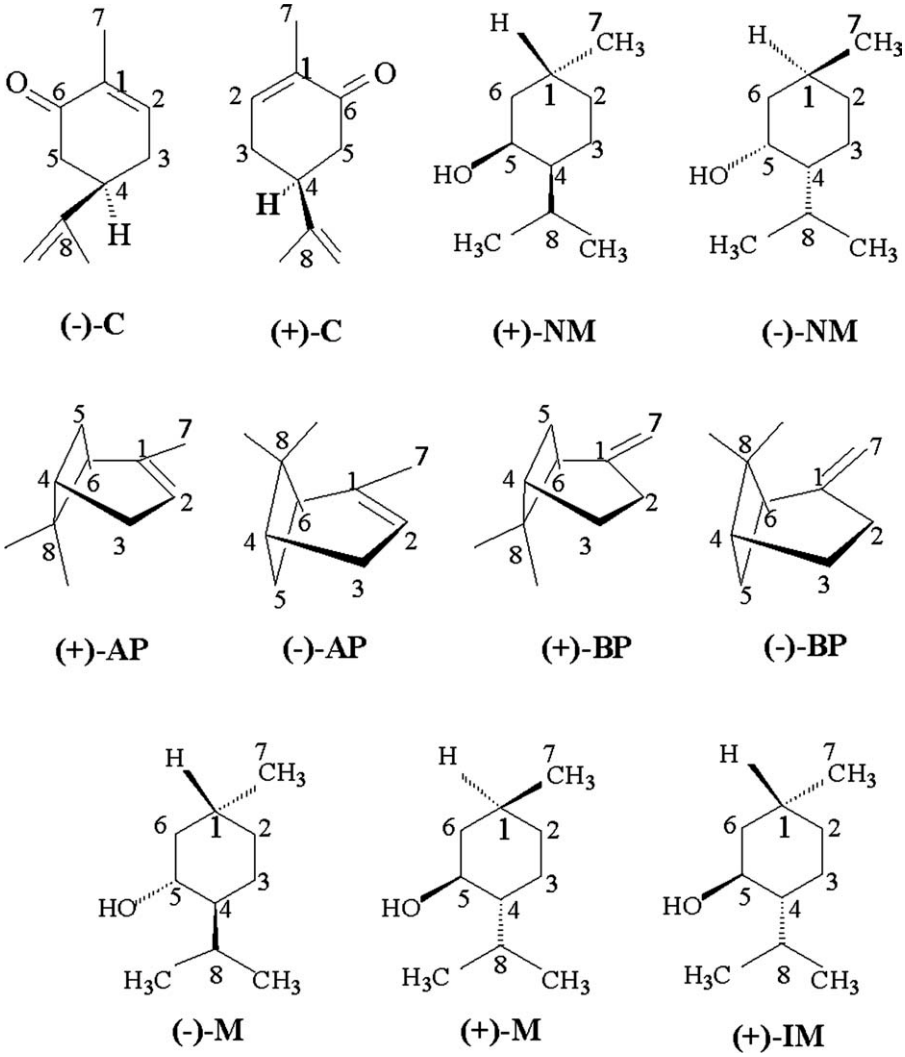

Fig. 1. Chemical structures of the monoterpenes studied in this work. Orthogonal views of the chemical structures of terpenes in the conformations of minimal energy in the vacuum. Numbers refer to C atoms equivalent within whole set of compounds studied. C, carvone; NM, neomenthol; AP, alpha-pinene; BP, beta-pinene; M, menthol; IM, isomenthol.

vertical and the emission polarizer horizontal (VH) or vice versa (HV). G is a correction factor for differences in sensitivity of the detection system for vertically and horizontally polarized light.[33]

With the purpose of evaluating the vesicles size change, the intensity of the light scattered by the vesicles suspension was recorded in a direction perpendicular to that of the incident light and both at the same wavelength ($\lambda = 356$ nm).

Anisotropy of DPH fluorescence at 430 nm ($\%\Delta A$) as well as the intensity of the 356-nm light dispersed ($\%\Delta LI_{356}$) were measured within a 0–2 mM concentration range of each of the MTs studied.

The values were expressed on a percent basis relatively to the control with ethanol, according to the following equation:

$$\%\text{Effect} = \frac{(\text{parameter})_{\text{sample}} - (\text{parameter})_{\text{control}}}{(\text{parameter})_{\text{control}}} \times 100.$$

Molecular Modeling and Calculation of Molecular Parameters

Molecular structures of the studied compounds were drawn using the molecular modeling program CS Chem3D 3.5.1. A modified version of Allinger's and the lowest energy 3D conformations of the molecules were determined using the energy minimization function of the program. Cosmo-solvation and semiempirical quantum mechanics calculation of molecular parameters was done with the MOPAC 3.5.1 module with MNDO potential function (Cambridge Soft Corporation, MA).

After energy minimization, the following molecular parameters were calculated for each molecule: hydrogen bond donor, hydrogen bond acceptor, surface tension, and dipole (it measures the asymmetry in the molecular charge distribution and is reported as a vector in three dimensions). In the same manner, dihedral angles (D ang constituted by carbon atoms indicated in Figure 1 and the electrostatic potential charges (EPChs) of these atoms were calculated.

The following molecular parameters were calculated with Marvin 5.3, 2010, ChemAxon software (http://www.chemaxon/marvfin/sketch/index.jsp): pK_a, polarizability, VDW (calculates the van der Waals surface of the molecule, in Å^2), chiral center, rotatable bound count (number of rotatable bonds in the molecule), polar surface area 2D at pH 7.4 (formed by polar atoms of a molecule), isoelectric point, refractivity (is strongly related to the volume of the molecules and to London dispersive forces that has important effect in drug–receptor interaction), and solvent-accessible surface area (SASA) (2D, pH 7.4, radii 1.4). While molar volume was calculated with PC model software.

On the other hand, log P (logarithm of the octanol/water partition coefficient) values were taken from Griffin et al.,[34] except those for neomenthols and menthols which were from Dambolena et al.[35]

All these molecular parameters are shown in Table 1.

TABLE 1. Molecular parameters of the MT studied, calculated with ChemAxo and PCmodel softwares

	Monoterpenes										
	Carvone		Menthol		Isomenthol	Neomenthol		α-Pinene		β-Pinene	
Molecular parameters	(+)	(−)	(+)	(−)	(+)	(+)	(−)	(+)	(−)	(+)	(−)
Log P[a]	2.74	2.74	3.32[b]	3.36[b]	3.19	2.87[b]	2.78[b]	4.44	4.48	4.16	4.16
Hydrogen bond donor[c]	0	0	1	1	1	1	1	0	0	0	0
Hydrogen bond acceptor	1	1	2	2	2	2	2	0	0	0	0
Surface tension[c]	29.8	29.8	29.7	29.7	29.7	29.7	29.7	25.3	25.3	27	27
Dipole (D)	3.41	3.24	1.53	1.61	1.52	1.58	1.66	0.09	0.08	0.35	0.35
pK_a[c]	0	0	19.55	19.55	19.55	19.55	19.55	0	0	0	0
Polarizability[c]	18.02	18.02	19.05	19.05	19.05	19.05	19.05	17.5	17.5	17.5	17.5
VDW (Å^2)[c]	248.28	246.52	312.98	313.29	313.26	311.71	311.68	255.46	255.49	253.55	253.52
Chiral center	1	1	3	3	3	3	3	3	3	3	3
Rotatable bound count[c]	1	1	1	1	1	1	1	0	0	0	0
Molar volume (cm^3)	131	133	175.5	175.5	175.5	175.5	175.5	125	124	124	126
Polar surface area[c]	17.07	17.07	20.23	20.23	20.23	20.23	20.23	0	0	0	0
Isoelectric point[c]	8.14	8.14	9.38	9.38	9.38	9.38	9.38	–	–	–	–
Refractivity	47.17	47.17	47.45	47.45	47.45	47.45	47.45	44.72	44.72	43.65	43.65
Solvent-accessible surface area at pH 7.4 (SASA)	310.45	301.47	332.44	333.24	318.66	310.63	310.35	292.74	292.24	274.52	274.53
D ang 6–1–2–3	−1.23	1.64	58.87	49.14	54.72	48.57	55.82	−1.76	1.79	−14.95	16.08
D ang 7–1–2–3	178.74	−179.37	−178.78	−78.02	−70.25	−76.88	178.66	178.48	−178.9	166.57	−165.17
D ang 2–1–6–5	−7.48	−9.13	−57.3	−44.18	−54.09	−50.09	−53.15	−45.96	45.79	−38.91	38.27
D ang 7–1–6–5	172.57	171.81	−179.68	82.25	70.98	75.21	−176.12	133.84	−133.59	139.56	−140.48
D ang 1–2–3–4[c]	−20.06	−19.62	−57.72	−57.41	−55.21	−54.64	−59.69	2.26	−2.03	14.63	−15.78
D ang 2–3–4–5	48.29	42.86	51.73	56.61	51.27	58.47	58.88	45.66	−45.97	39.43	−38.85
D ang 3–4–5–6[c]	−56.92	−50.55	−49.31	−50.27	−49.78	−60.4	−55.52	−83.89	84.07	−85.37	85.23
D ang 4–5–6–1	36.82	34.4	53.73	45.91	53.2	58.13	53.65	82.88	−82.79	84.48	−84.37
EPCh 1	−0.01	−0.07	0.28	0.28	0.39	0.25	0.35	−0.05	0.01	0.01	0.02
EPCh 2	−0.18	−0.06	−0.37	−0.29	−0.55	−0.32	−0.44	−0.15	−0.15	−0.22	−0.24
EPCh 3[c]	−0.32	−0.46	−0.34	−0.22	−0.08	−0.28	−0.12	−0.43	−0.43	−0.41	−0.4
EPCh 4[c]	0.2	0.17	0.11	−0.4	−0.07	−0.27	−0.38	0.03	0.03	0.01	−0.01
EPCh 5	−0.62	−0.48	0	0.17	0.25	0.19	0.06	−0.45	−0.44	−0.42	−0.41
EPCh 6	0.37	0.38	−0.49	−0.46	−0.62	−0.51	−0.63	0.01	−0.01	−0.08	−0.1
EPCh 7	−0.56	−0.57	−0.63	−0.62	−0.6	−0.58	−0.6	−0.5	−0.51	−0.47	−0.47

[a]Values are taken from Ref. [34].

[b]Values are taken from Ref. [35]. VDW, van der Waals. Numbers and values of dihedral angles (D ang) and electrostatic potential charge (EPCh) refer to C atoms in Figure 1.

[c]Variables not used in PCA because of their high correlation with log P or with D ang or EPCh values (see text).Abbreviations: %ΔA, anisotropy change percent; %ΔLI_{356}, light intensity at 356-nm change percent; (−)-AP, (−) α-pinene; (+)-AP, (+) α-pinene; (−)-BP, (−) β-pinene; (+)-BP, (+) β-pinene; (−)-C, (−) carvone; (+)-C, (+) carvone; DPH, diphenylhexatriene; dpPC, dipalmitoylphosphatidylcholine; FI, fluorescence intensity; Gr., group; (+)-IM, (+) isomenthol; LUVs, large unilamellar vesicles; (−)-M, (−) menthol; (+)-M, (+) menthol; MLVs, multilamellar vesicles; MT, monoterpene; (−)-NM, (−) neomenthol; (+)-NM, (+) neomenthol; $P_{o/w}$, octanol/water partition coefficient; PCA, principal component analysis; VDW, van der Waals area for solvation.

Statistical Analysis

All data were statistically analyzed using statistical InfoStat software.[36] Hierarchical cluster analysis was carried out based on the anisotropy and light scattering data of all the MTs and their racemic mixtures. For this study, we used the "average linkage" clustering algorithm and "Standar Euclidean distance."

Principal component analysis (PCA) was then performed on the molecular property data to determine which parameters most contributed to the conformation of the groups (based on the prior classification obtained by the hierarchical cluster analysis, but without the control and racemic mixtures).

Pearson correlation coefficients (r) were calculated to find relationships among the different molecular parameters and used to reduce the number of variables in the data matrix of PCA. Therefore, those molecular parameters exhibiting high r ($\geq$0.95), when compared with "log P" value or other parameters, were not included in the PCA.

RESULTS

Chemical structures of MTs used are shown in Figure 1. Equivalent carbon atoms among all the MTs in Figure 1 were identified with arbitrary arabic numbers. According to their characteristic functional groups, the molecules studied were classified as hydrocarbons (α- and β-pinenes), alcohols (menthols), or ketones (carvone).

As the effects of the terpenes could be traced to functions localized at the membranes of organisms,[5,28,37–39] this general interaction might be evidenced by the measurement of fluorescence polarization of DPH as an indicator of possible changes in membrane microviscosity.

Effect of Monoterpenes on DPH Fluorescence Anisotropy in Bilayer Membranes

Figure 2 (left panels) shows the variation in the percentual change in the fluorescence anisotropy at 430 nm with respect to the control (at the same ethanol concentration) (%ΔA), taken as a measure of change in membrane order and dynamics. The variation in the percentual change in light intensity (LI) at 356 nm with respect to the control sample (%ΔLI_{356}) (Fig. 2, right panel) was the light scattered and reflected changes in the dpPC vesicles size.

In the absence of MTs, the DPH fluorescence anisotropy values obtained ($A_{DPH} \cong 0.33$) corresponded to that of a bilayer organized in a gel phase in which the hydrocarbon chain region imposed constraints to changes in the probe's order and mobility.[32,40] Upon increasing the MTs concentration, the anisotropy values decreased up to $A \cong 0.210$, reflecting a membrane disorganizing process through a transition from the gel to liquid crystalline phase of dpPC, which was not completed in the membrane model used (LUVs) and within the MTs concentration range assayed. The latter phase organization measured in MLVs was characterized by an $A_{DPH} = 0.125$, and these values could be reached in the presence of ~1.3 mM *ortho*-nitrophenol, which is known to locate at the polar head group region of the bilayers.[30] It was shown that MTs bearing different functional groups exhibited a concentration-dependent decreasing trend in %ΔA with the following sensitivity sequence: hydrocarbons >> alcohols (except IM) > ketones. Moreover, %ΔA values showed a high positive correlation with octanol/water partition coefficients (Table 1).

In general, the (−) stereoisomers of NM, C, and AP were less effective at decreasing A than their (+) isomers (Figs. 2b, 2d, and 2e). The opposite was observed with β-pinenes,

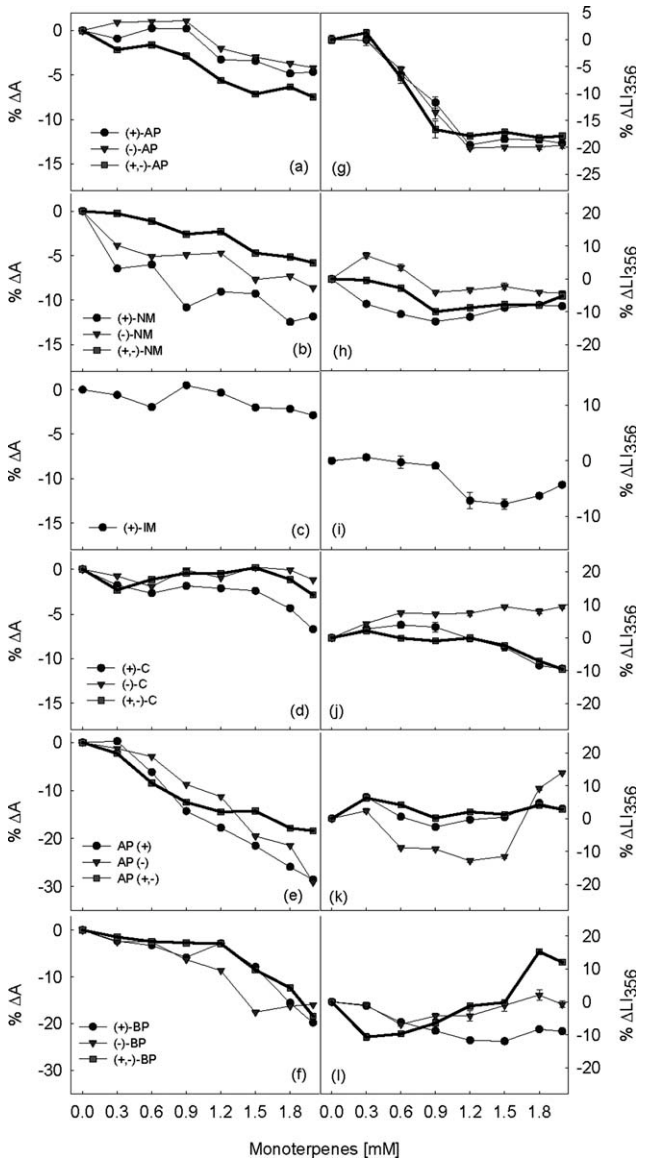

Fig. 2. Enantioselectivity of DPH anisotropy and light scattering changes in dpPC bilayers induced by monoterpenes enantiomers and their racemic mixtures. %ΔA, variation of the percent change in anisotropy (**a–f**) and %LI_{356}, percent change in the intensity of the 356-nm light scattered (**g–l**) with respect to the corresponding control, as a function of the monoterpene concentration. Control sample was prepared in the absence of MT and contained ethanol at the same concentration used as a vehicle of MT in the corresponding experimental sample. Points represent the mean of at least four determinations.

being (−)-BP more active than (+)-BP (Fig. 2f), whereas (+)-M and (−)-M exhibited a similar potency (Fig. 2a).

(±)-M showed a potentiated effect with respect to (+)-M and (−)-M alone. The racemic mixture of NM was less potent than the individual stereoisomers at decreasing A, which suggested a clear antagonistic effect between (−)-NM and (+)-NM. In the case of C and BP, the activities of racemates were lower than that of (+) or that of (−), respectively. Hence, the activities in the mixture deviated toward that of the (−)-C or (+)-BP. In the case of AP, the relative intensity of the racemate compared with that of the individual stereoisomers was bimodal, with an enhancement in the disorganizing effect below and an antagonistic effect above 1.35 mM, respectively.

Effect of Monoterpenes on the Intensity of Light Scattered by Phospholipid Vesicles Size

To investigate if the disordering effects induced by MTs could proceed toward a disruption of the vesicles structure, the intensity of light scattering induced by the samples was measured at the same wavelength (356 nm) but at a perpendicular direction with respect to the incident light. The effect of MTs on $\%\Delta LI_{356}$ is depicted in Figure 2 (right panels).

The general trend observed was a decreasing intensity of the light scattered as a function of MT concentration at a maximum $\%\Delta LI_{356}$ of −20 and −12% in the case of menthols (Fig. 2g) and (+)-BP (Fig. 2l), respectively, whereas (−)-C (Fig. 2j) increased the light scattering within the whole range of concentrations assayed, being an exception to this rule.

Two types of biphasic behaviors were observed: in the case of (−)-NM, (+)-AP, and (±)-AP, which showed an increase in the light scattered at the lowest concentrations previous to acquire the decreasing trend, and (+)-NM, (−)-AP, and (±)-BP which after reaching a minimum in the light scattering at 0.9–1.2 mM (the two first) or at 0.3 mM (the latter) started increasing at higher MT concentrations (Figs. 2k and 2l).

Following a similar rational applied to the interpretation of MTs effect on fluorescence anisotropy, the effect of racemates on the intensity of light scattering can be compared with that of individual enantiomers. An antagonism was observed in the cases of NM, C, and also with AP at low concentration, showing a deviation of the effect toward that of the (+)-enantiomer behavior, which in the two first MTs had a higher disorganizing effect than the (−)-enantiomer and the contrary occurred with the latter. A potentiation was observed with the (±)-BP if compared with the single enantiomers, enhancing the disordering effect or leading to an ordering effect at low and high concentrations, respectively.

Cluster Analysis

Hierarchical cluster analysis was based on anisotropy and light scattering data and was carried out at low, medium, and high MTs concentrations (0.3, 1.2, and 2 mM). This analysis showed that at low MT concentrations (Fig. 3a) all the MTs and their racemic mixtures arranged into three groups, whereas at medium (Fig. 3c) and high (Fig. 3e) MT concentrations, samples distributed within five and six different groups, respectively.

At low MT concentration (Fig. 3a), in Gr. 2, the racemic mixture of BP had the highest light scattering change (−11%) and (+)-NM (Gr. 1) showed the highest $\%\Delta A$ (−6.5%) (see Fig. 4a). Gr. 3 included the rest of the terpenes that did not differed from the control. However, (−)-NM and (±)-AP as well as (−)-C and (+)-AP, which were included into two subgroups of Gr. 3, were characterized by a high and positive light scattering change (between 4.3 and 7.2%) (Fig. 4a).

At medium MT concentration (Fig. 3c), (−)-C (Gr. 2) is the only terpene that had a high positive light scattering change (7.5%) and did not affect the anisotropy (Fig. 4b). Gr. 1 [(+)-AP and (±)-AP] contained the terpenes with the highest effect on $\%\Delta A$ (−17.8 and −14.5%, respectively). Gr. 4 [menthols], included the MTs with the highest values in $\%\Delta LI_{356}$ (−18 to −20%), and Gr. 5 [(−)-BP, (+)-NM, and (−)-AP] were characterized by a $\%\Delta A \cong -10\%$ (Fig. 4b). The behavior of the rest of the MT in the Gr. 3 was closed to that of the control; hence, they exhibited the lowest changes.

At the highest MT concentration studied (2 mM, Fig. 3e), (−)-C (Gr. 3) was characterized by a high and positive light scattering change ($\%\Delta LI_{356} = 9.5\%$) and had no effect on the anisotropy. Menthols were in Gr. 1 and showed the highest change in light scattering data (−18 to −19.6%). (±)-BP, included in Gr. 5, and both the enantioisomers of AP in Gr. 6 showed a high change in both anisotropy and light scattering data (≅19 and ≅29%, respectively) (Fig. 4c).

Pearson Correlation Analysis and Principal Component Analysis

PCA was then applied to ascertain which molecular property (Table 1) or combination of molecular properties of the MTs were associated with these different activity patterns showed in the groups formed previously (see letter Groups in Figs. 3a, 3c, and 3e). Before doing the PCA, Pearson correlation coefficients (r) were calculated both to find relationships between the different molecular parameters and to reduce the number of variables in the data matrix of PCA. Therefore, those molecular parameters that resulted highly correlated (high $r \geq |0.90|$) with "log P" value or with other parameters (high $r \geq |0.95|$) were not used for PCA. Hence, the following molecular properties were not used in the PCA: surface tension, rotatable bound count, isoelectric point, hydrogen bond donor, EPCh 3, 4, and 7, pK_a, polarizability, VDW, polar surface area, and D ang 1-2-3-4 and 3-4-5-6.

PCA was applied to each of the three MT concentration used in the previous cluster analysis. The contribution of the molecular parameter to a specific component is reflected by the loading value derived from PCA analysis. Those molecular parameters with the highest loading values were considered to have the strongest influence on the value of the respective principal component.

In the PCA for 0.3 mM MT concentration (Fig. 3b) the first two PCs explained 100% of total variance. The first component, which explains 87% of total variance, was mainly influenced (loading values $> |0.26|$) by variables log P ($K_{o/w}$), hydrogen bond acceptor, dipole, EPCh 6, chiral center, molar volume, refractivity, SASA, and D ang 6-1-2-3, 2-1-6-5, and 2-3-4-5. PC1 separated Gr. A and B (NM enantioisomers) from Gr. C (the rest of the MTs). NM enantioisomers were characterized by the highest D ang 2-3-4-5 of 58°. PC2 divided Gr. A [(+)-NM] from Gr. B [(−)-NM] mainly and is influenced by variables D ang 7-1-2-3 and D ang 7-1-6-5, which have values of dissimilar in magnitude and opposite signs between one another (Table 1).

The first two components of PCA for 1.2 mM encompassed 77% of the total variance from this data set (Fig. 3d). The first component accounted for 48% of the variance and allowed distinction of Gr. A [(+)-AP] and B [(−)-C], mainly from the other groups. It was influenced by the followed variables: EPCh1 (the lowest and negative values), EPCh5 (the highest and negative), molar volume, and D ang 6-1-2-3 (lower value ≅ |1.7|). Gr. C and Gr. E, which included mainly pinenes, IM, and NM, were characterized by high values of log P. The PC2 allowed distinction of Gr. B [(−)-C] from the rest and was separated by log P (the lowest value) and dipole (the highest value).

At the maximum MT concentration studied (2 mM), examination of the scores and loading plots for PC1 versus PC2 (96% of the variance) showed that Gr. B [(−)-C] was clearly

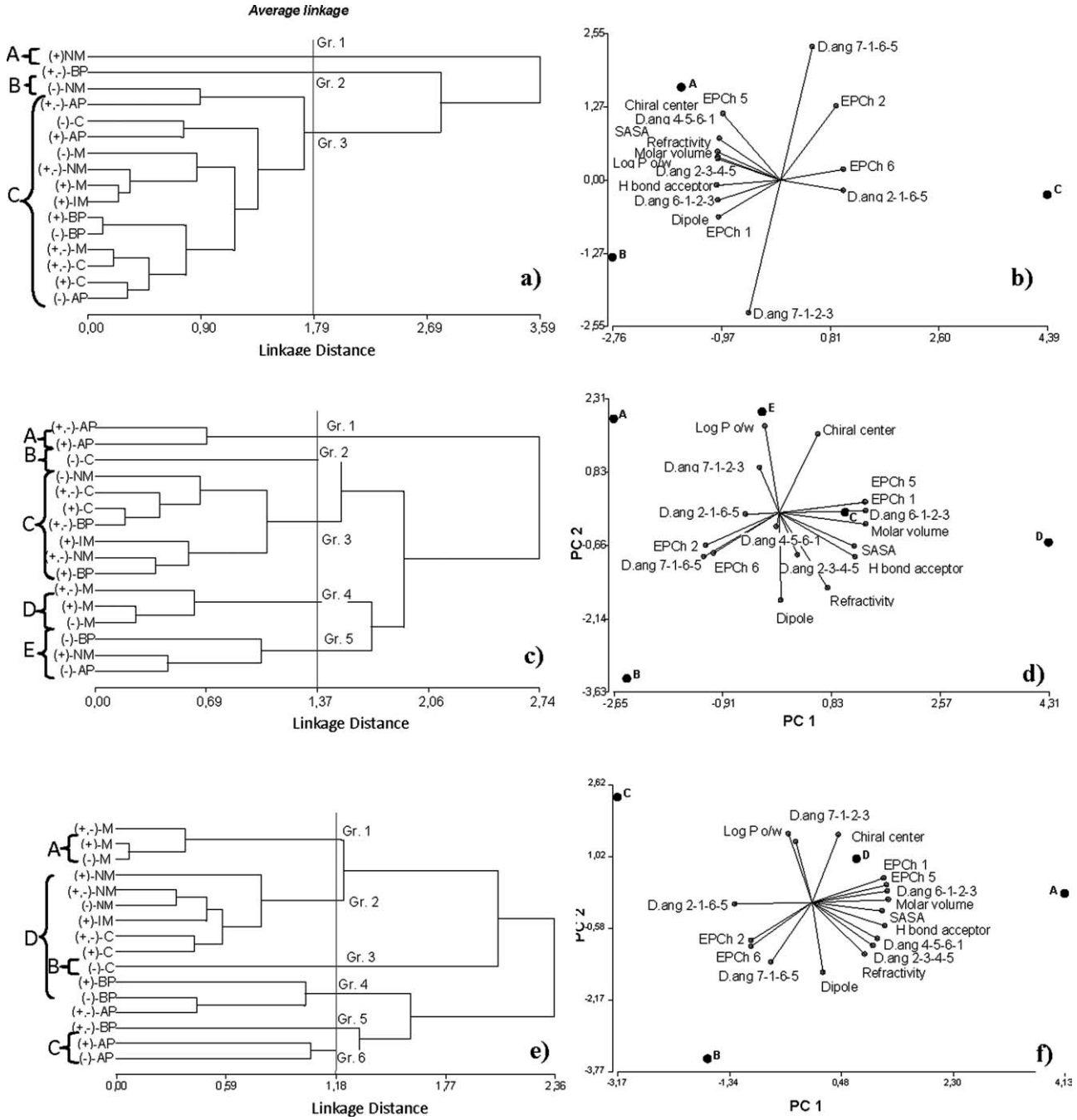

Fig. 3. Hierarchical clustering and principal component analysis based on experimental and theoretical properties of monoterpenes and their racemic mixtures. (**a**, **c**, and **e**) Hierarchical cluster analysis based on anisotropy and light scattering data. Racemic mixtures and controls were not included in Groups A, B, C, and D. Names marked with bold and italic letters refer to the compounds left for PCA analysis. (**b**, **d**, and **f**) PCA on Groups A–D and the variables shown in Table 1. Score plots of molecular parameters and Groups A–D of MTs enantiomers derived from the cluster analysis into the plane defined by the first two principal components (PC1 against PC2) for different MTs. Each analysis was performed at three different MT concentrations (a, b: 0.3 mM; c, d: 1.2 mM; e, f: 2 mM).

separated from the rest of the other groups (Fig. 3f). The molecular parameters that made the highest contribution to such separation in the PC2 were log *P*, dipole, and chiral center (the lowest value).

The hydrocarbons AP (Gr. C) were mostly separated from menthols (Gr. A) by the principal component 1 of PCA, which accounted for 60% of the total variance (Fig. 3f). The variables that characterized this component were hydrogen bond acceptor character (absent in pinenes), EPCh5 (higher for pinenes than for menthols), and molar volume (pinenes presented the lowest values).

DISCUSSION

A representative phospholipid dpPC has been widely used to formulate model biomembranes. This zwitterionic amphipathic phospholipid spontaneously aggregates into bilayers forming multilamellar (MLVs) upon dispersing in water

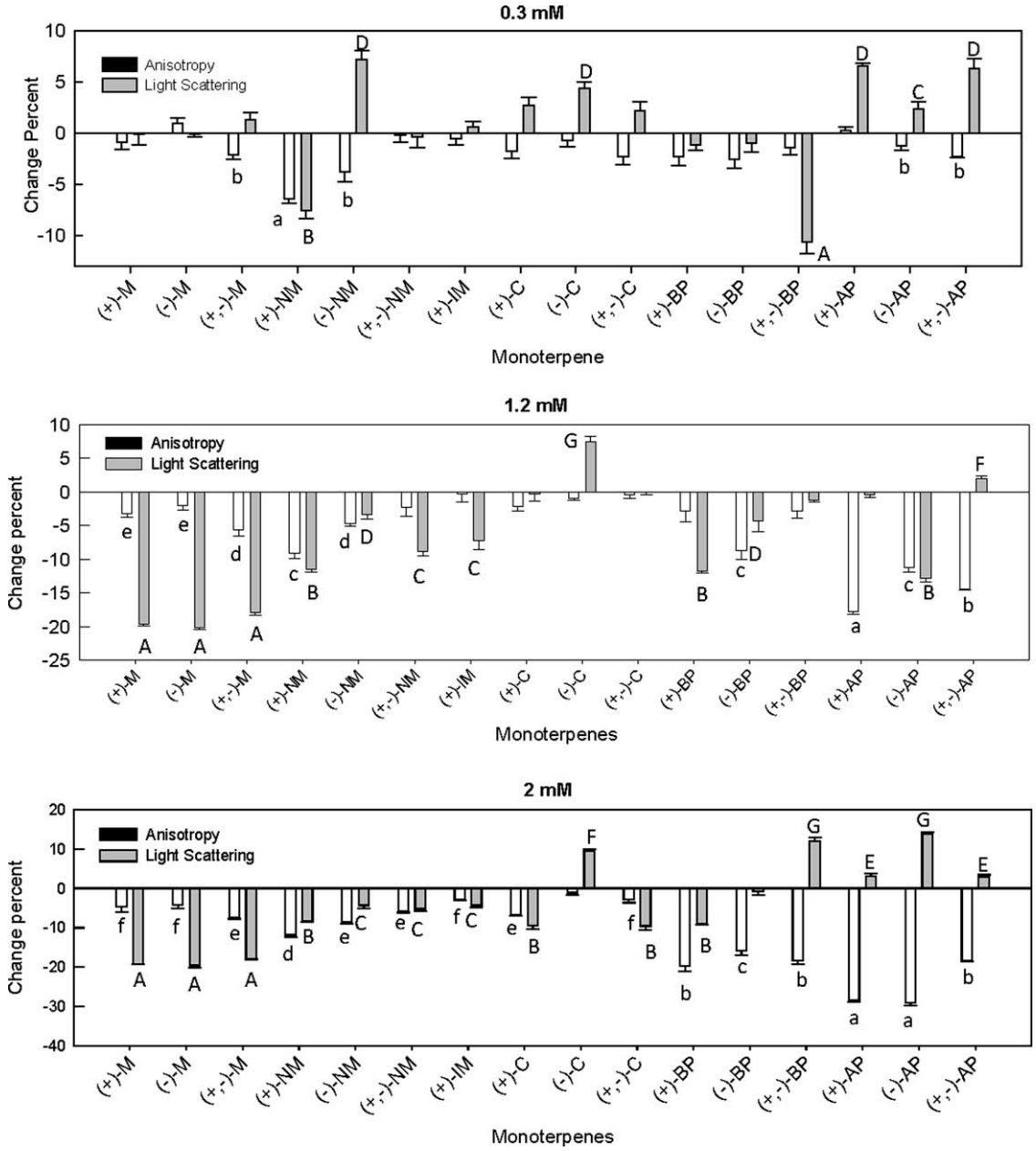

Fig. 4. Effect of MTs at three concentrations (**a**: 0.3 mM; **b**: 1.2 mM, and **c**: 2 mM) on DPH fluorescence anisotropy and light scattering of dpPC self-aggregating structures. Letters denote significant difference between treatment and control for each variable. Bars having different capital letters (light scattering) or small letters (anisotropy) are significantly different between one another according to Duncan's multiple range test at $P < 0.05$ ($n = 4$).

above a critical micellar concentration. In turn, MLVs, depending on the subsequent treatment they receive, can give rise to unilamellar vesicles of different sizes. LUVs are usually preferred to be used with spectroscopy techniques instead of MLVs because of their lower light scattering effect. Below 41°C, the main phase transition temperature, the dpPC bilayer consists in a gel phase. The phase behavior of dpPC bilayer membrane has been studied in the presence of some molecules that partition therein. For example, ethanol-induced effects have been attributed to a transition from the bilayer phase to a kind of gel phase in which the lipid acyl chains from opposing leaflets are fully interdigitated.[41]

Changes in the molecular organization at the polar head group level of bilayers (e.g., hydration) may be transmitted to the hydrocarbon chain core region[42] affecting general membrane properties such as molecular order and dynamics reflected through the microviscosity.

The hydrophobicity of MTs allows the prediction of their action at the level of the membrane and membrane-embedded proteins.[43,44]

A direct relationship can be found between the amount of a particular partitioned compound and its effect on the structural integrity and functional properties of membranes. However, the type of hydrophobic interaction and the depth within the membrane where the lipophilic compound resides will determine the extent to which the membrane will be expanded,[45,46] the correlation between the extent of expansion and the molar volume of the compound,[47] as well as the extraction of phospholipids through budding transformation.[48] The latter depends on the interplay of spontaneous

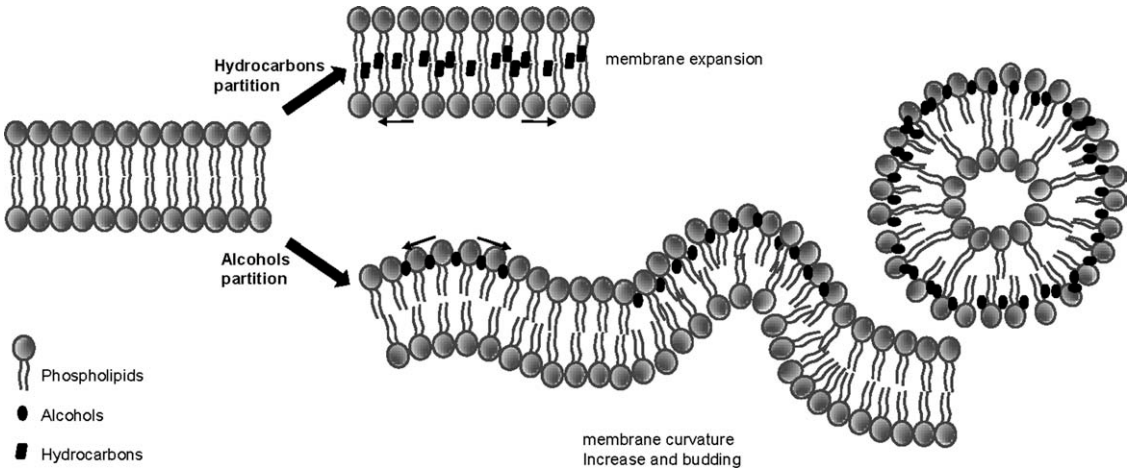

Fig. 5. Localization-dependent changes induced by monoterpenes on the membrane bilayer organization. Monoterpenes belonging to the group of hydrocarbons localized within the hydrocarbon membrane core inducing a membrane expansion and stiffening, evidenced by the increase in light scattering and decrease in anisotropy at the highest concentrations. Alcohols localized within the polar head group membrane region inducing a curvature increase, which in turn leaded to the production of low-size LUVs through a budding process, evidenced by a decrease in light scattering and a slight change in fluorescence anisotropy.

curvature, bending rigidity, and line tension within a fluid membrane domain that may be induced by drug accumulation.[45–48]

It is noteworthy that at low concentrations NMs showed enantioselectivity, whereas the rest of the MTs tested did not. At low concentration, NMs affected mainly the anisotropy and showed a different behavior between them with regard to light scattering, while the (−)-NM induced an increase and (+)-NM decrease it (Fig. 4a). The molecular characteristics that allowed separate them were mainly EPCh5, EPCh2, D ang 7-1-2-3, and D ang 7-1-6-5 (the latters exhibit values that are very different from each other and had opposite signs). This enantioselectivity was lost at the highest concentrations probably because the bilayer membrane structure may have been affected at a high extent.

On the other hand, it should be noted that Ms did not show that enantioselectivity, though remained together in clustered groups at all concentrations studied. However, they also showed large differences in the D ang 7-1-2-3 and 7-1-6-5, which could separate NMs. The most prominent molecular differences between menthols and neomenthols were the log *P* (higher in the formers) and the SASA (somewhat lower in the latter). The main structural difference among menthols is the orientation of substituent in the quiral carbon atoms C1, C4, and C5, which are all equatorial in M, axial in C1, and equatorial in C4 and C5 in the case of IM, and axial in C1 and C4 and an equatorial orientation at C5 in NM. This would explain the lowest value for SASA in the later. At low concentration, the behavior of (−)NM differs from other menthols; moreover, (+)-NM and (−)-NM also differ in the values for EPCh 1and EPCh 4.

Another feature to note is the unique effect of (−)-C regarding the increase of particles size (high positive values of dispersion) over all concentrations. This could be because this terpene had a partial flat configuration compared with the other terpenes studied and could be "stacked" and fit better within the membrane core inducing a membrane expansion without breaking the bilayers structure. It is not clear why (+)-C, having molecular characteristics similar to those of its isomer, did not show the same trend. The stronger differences between (−)-C and (+)-C can be that (−)-C has in the quiral C4 carbon, whereas the isopropyl is in the axial orientation in (−)-C, in (+)-C it is equatorial which confers a more planar conformation. This is also supported by the dihedral angles D ang 6,5,4,8 (being C6 the carbonyl carbon atom), which is 74.76° for (−)-C and −177° for (+)-C and D ang 2,3,4,8, which is −84° and 172° for (−)-C and (+)-C, respectively. Hence, (+)-C exhibits nearly planar surfaces (angles close to 180°) characteristic of equatorially oriented substituents or due to conjugated double bonds such as in the carbonylic oxygen (O) 6,1,2 with D ang 173.5°. Moreover, D ang 6-1-2-3 and 7-1-2-3 with opposite directions and the largest difference in EPCh values in atoms 1, 2, 3, and 5 force it to present a more external localization within the membrane depth. Phospholipids composing the model membrane are also chiral molecules and were present as a racemic mixture. Hence, carvones may have the ability of distinguishing between chiral mesoscopic structures (membrane domains) depending on the structural nature of the stereoisomer. This hypothesis is currently under investigation in our laboratory.

The membrane expansion induced by C did not lead to a membrane stiffering as evidenced by the decrease in anisotropy. This behavior, which may be rationalized as a disruption of the crystalline structure, resembles the effect of cholesterol in disordering bilayers originally organized in the gel phase (note that cholesterol, as well as (+)-C, possesses a planar molecular structure, and its dual effect on bilayers organization, disordering the gel phase and ordering the fluid phase, is widely accepted[49]).

On the other hand, menthols showed the highest effect on decreasing the dispersion levels. This could be associated to their higher molar volume and their more globular (not flat) molecular structure, which leaded to a disruption of the membrane structure through a budding transformation upon their accumulation within the membrane polar head group region leading to a lowering of the particles' size.

Pinenes, mainly alpha rather than beta, with the smaller molar volume, had the greatest effect on the anisotropy at higher concentrations. This would allow the accumulation of a higher amount of molecules inside the membrane without reaching to a disruption reflecting at the same time their high lipophilicity (high partition coefficient).

As a generalization, schematized in Figure 5, it can be concluded that the behavior of the less polar compounds (hydrocarbons) was characterized by a membrane expansion (increase in light scattering) detectable within the low concentration range and by their permanence in the membrane up to the highest concentrations tested that allowed they exhibiting a concentration-dependent anisotropy decrease. In turn, with the more polar terpenes (alcohols) it prevailed the production of higher amounts of low-size LUVs (more evident at the medium and high concentration ranges) with roughly constant curvature, which explains the slight change in microviscosity (A_{DPH} anisotropy). These behaviors can be rationalized according to the deeper localization within the membrane core of the formers compared with the latters, which can be predicted from the corresponding polar charge distribution in their molecular structures. Consistently, menthols, which have the biggest molar volume among the studied monoterpenos and are good hydrogen bond donors and acceptors (Table 1), are expected to be trapped at the polar head group membrane region and resulted more effective than other compounds with smaller molar volumes at inducing a decrease in light scattering.

The enantioselectivity was expressed by NM at low concentration and by C and pinenes at medium concentration. Inhibition and potentiation were evidenced, within the low concentration range, by the racemic mixtures in NM and BP, respectively. These effects might be related with a nonideal behavior of the racemic mixtures, which might exhibit condensation due to electrostatic interaction in the case of NM or expansion due to steric hindrance in the case of BP.

Usually, in the field of drug–membrane interactions, most studies were mainly focused on ligand–receptor interactions and docking leading to define the pharmacological and biological stereoselective effects and predictions of structure–activity relationships. It is interesting to recall that menthol within a concentration range 0–1 mM exhibited enantioselectivity at stimulating a benzodiazepine (BZD) binding to $GABA_A$ receptor ((+)-M was active but (−)-M was not).[20] Analyzing this behavior in conjunction with the results obtained in this work, it is possible to hypothesize the resolution of two action levels of menthol. One of them partitioning at the polar head group region and inducing the production of small vesicles through a budding process. This provides the scaffold for a $GABA_A$-receptor conformation with higher activity for BZDs than lower curvature environments and which expressed the enantioselectivity for (+)-M. (+)-NM also tended to show a stronger effect than its (−)-NM isomer at activating BZD binding but at concentrations so high that the enantioselectivity for the structural effects reported here would have already been lost.

CONCLUSION

Consequently, in view of the dynamic organization of membrane, stereospecificity becomes a relative concept because of its environmental dependence; thus, the reductionist perspective that considers the receptor activity and binding capacity dependent only on the interaction between two molecular entities (drug and receptor) is not enough to describe structure–activity relationships.[22] In this context, the importance of the chirality of the terpenes on its interaction with a chiral membrane environment remains to be elucidated.

Chirality DOI 10.1002/chir

ACKNOWLEDGMENTS

MPZ, AVT, JAZ, and MAP are career investigators from CONICET.

LITERATURE CITED

1. Rauha JP, Remes S, Heinonen M, Hopia A, Kahkonen M, Kujala T, Pihlaja K, Vuorela H, Vuorela P. Antimicrobial effects of Finnish plant extracts containing flavonoids and other phenolic compounds. Int J Food Microbiol 2000;56:3–12.
2. Koroch A, Juliani H, Zygadlo J. Bioactivity of essential oils and their components. In: Berger RG, editor. Flavours and fragrances: chemistry, bioprocessing and sustainability. Berlin: Springer-Verlag; 2007. p 87–103.
3. Lahlou M. Methods to study the phytochemistry and bioactivity of essential oils. Phytother Res 2004;18:435–448.
4. Griffin S, Wyllie S, Markham J, Leach D. The role of structure and molecular properties of terpenoids in determining their antimicrobial activity. Flavour Fragr J 1999;14:322.
5. Cristani M, D'Arrigo M, Mandalari G, Castelli F, Sarpietro MG, Micieli D, Venuti V, Bisignano G, Saija A, Trombetta D. Interaction of four monoterpenes contained in essential oils with model membranes: implications for their antibacterial activity. J Agric Food Chem 2007;55:6300–6308.
6. Zunino MP, Zygadlo JA. Effect of monoterpenes on lipid oxidation in maize. Planta 2004;219:303–309.
7. Zunino MP, Zygadlo JA. Changes in the composition of phospholipid fatty acids and sterols of maize root in response to monoterpenes. J Chem Ecol 2005;31:1269–1283.
8. Sikkema J, Weber F, Heipieper H, de Bont JAM. Cellular toxicity of lipophilic compounds: mechanisms, implications, and adaptations. Biocatalysis 1994;10:113–122.
9. Turina AV, Perillo MA. Monoterpenes affect chlorodiazepoxide-micelle interaction through micellar dipole potential modifications. Biochim Biophys Acta 2003;1616:112–120.
10. Turina AV, Nolan MV, Zygadlo JA, Perillo MA. Natural terpenes: self-assembly and membrane partitioning. Biophys Chem 2006;122:101–113.
11. Sikkema J, de Bont J, Poolman B. Mechanisms of membrane toxicity of hydrocarbons. Microbiol Rev 1995;59:201–222.
12. Ultee A, Kets EPW, Smid EJ. Mechanisms of action of carvacrol on the food-borne pathogen *Bacillus cereus*. Appl Environ Microbiol 1999;65:4606–4610.
13. Srivastava IK, Rottenberg H, Vaidya AB. Atovaquone, a broad spectrum antiparasitic drug, collapses mitochondrial membrane potential in a malarial parasite. J Biol Chem 1997;272:3961–3966.
14. Sikkema J, Poolman B, Konings WN, de Bont JA. Effects of the membrane action of tetralin on the functional and structural properties of artificial and bacterial membranes. J Bacteriol 1992;174:2986–2992.
15. Ferté J. Analysis of the tangled relationships between P-glycoprotein-mediated multidrug resistance and the lipid phase of the cell membrane. Eur J Biochem 2000;267:277–294.
16. Lawrence B. Essential oils: from agriculture to chemistry. Int J Aromather 2000;10:82–98.
17. Lanier G, Classon A, Stewart T, Piston J, Silverstein R. Ips pini: the basis-for interpopulational differences in pheromone biology. J Chem Ecol 1980;6:677–687.
18. Stranden M, Borg-Karlson AK, Mustaparta H. Receptor neuron discrimination of the germacrene D enantiomers in the moth *Helicoverpa armigera*. Chem Senses 2002;27:143–152.
19. Heuberger E, Hongratanaworakit T, Bohm C, Weber R, Buchbauer G. Effects of chiral fragrances on human autonomic nervous system parameters and self-evaluation. Chem Senses 2001;26:281–292.
20. Corvalan NA, Zygadlo JA, Garcia DA. Stereo-selective activity of menthol on GABA(A) receptor. Chirality 2009;21:525–530.
21. Vokou D, Douvli P, Blionis GJ, Halley JM. Effects of monoterpenoids, acting alone or in pairs, on seed germination and subsequent seedling growth. J Chem Ecol 2003;29:2281–2301.
22. Perillo M. The drug-membrane interaction: its modulation at the supramolecular level. In: Condat CA, Baruzzi A, editors. Recent research development in biophysical chemistry. Trivandrum: Research Signpost; 2002;106–121.

23. Perillo M, Zygadlo J. Terpenes. Stereochemistry and bioactivities. Curr Top Phytochem 2005;7:89–104.
24. Eichelbaum M. Enantiomers: implications and complications in developmental pharmacology. Dev Pharmacol Ther 1992;18:131–134.
25. McIntosh TJ, Simon SA. Roles of bilayer material properties in function and distribution of membrane proteins. Annu Rev Biophys Biomol Struct 2006;35:177–198.
26. Powl AM, East JM, Lee AG. Importance of direct interactions with lipids for the function of the mechanosensitive channel MscL. Biochemistry 2008;47:12175–12184.
27. Garcia DA, Perillo MA. Benzodiazepine localisation at the lipid-water interface: effect of membrane composition and drug chemical structure. Biochim Biophys Acta 1999;1418:221–231.
28. Uribe S, Ramirez J, Pena A. Effects of beta-pinene on yeast membrane functions. J Bacteriol 1985;161:1195–1200.
29. Ricchelli F, Camerin M, Beghetto C, Crisma M, Moretto V, Gobbo S, Salvato B, Salet C, Moreno G. Disaccharide modulation of the mitochondrial membrane fluidity changes induced by the membrane potential. IUBMB Life 2001;51:111–116.
30. Sanchez JM, Turina AV, Perillo MA. Spectroscopic probing of ortho-nitrophenol localization in phospholipid bilayers. J Photochem Photobiol B 2007;89:56–62.
31. Shrivastava S, Paila YD, Dutta A, Chattopadhyay A. Differential effects of cholesterol and its immediate biosynthetic precursors on membrane organization. Biochemistry 2008;47:5668–5677.
32. Kaiser RD, London E. Location of diphenylhexatriene (DPH) and its derivatives within membranes: comparison of different fluorescence quenching analyses of membrane depth. Biochemistry 1998;37:8180–8190.
33. Bangham AD, Hill MW, Miller NGA. Preparation and use of liposomes as models of biological membranes. In: Korn ED, editor. Plenum: New York; Methods in Membrane Biology. 1974. p1–68.
34. Griffin S, Wyllie SG, Markham J. Determination of octanol-water partition coefficient for terpenoids using reversed-phase high-performance liquid chromatography. J Chromatogr A 1999;864:221–228.
35. Dambolena JS, López AG, Rubinstein HR, Zygadlo JA. Effects of menthol stereoisomers on the growth, sporulation and fumonisin B1 production of *Fusarium verticillioides*. Food Chem 2010;123:165–170.
36. InfoStat. InfoStat versión 1.1. Argentina: Grupo InfoStat F, Universidad Nacional de Córdoba; 2002.
37. Trombetta D, Castelli F, Sarpietro MG, Venuti V, Cristani M, Daniele C, Saija A, Mazzanti G, Bisignano G. Mechanisms of antibacterial action of three monoterpenes. Antimicrob Agents Chemother 2005;49:2474–2478.
38. Bard M, Albrecht MR, Gupta N, Guynn CJ, Stillwell W. Geraniol interferes with membrane functions in strains of Candida and Saccharomyces. Lipids 1988;23:534–538.
39. Abrahim D, Braguini WL, Kelmer-Bracht AM, Ishii-Iwamoto EL. Effects of four monoterpenes on germination, primary root growth, and mitochondrial respiration of maize. J Chem Ecol 2000;26:611–624.
40. Engel LW, Prendergast FG. Values for and significance of order parameters and "cone angles" of fluorophore rotation in lipid bilayers. Biochemistry 2002;20:7338–7345.
41. Zeng J, Chong PLG. Interactions between pressure and ethanol on the formation of interdigitated DPPC liposomes: a study with Prodan fluorescence. Biochemistry 1991;30:9485–9491.
42. Milhaud J. New insights into water-phospholipid model membrane interactions. Biochim Biophys Acta 2004;1663:19–51.
43. Sikkema J, de Bont J, Poolman B. Interactions of cyclic hydrocarbons with biological membranes. J Biol Chem 1994;269:8022–8028.
44. Hamill OP, Martinac B. Molecular basis of mechanotransduction in living cells. Physiol Rev 2001;81:685–740.
45. Perillo MA, Garcia DA. Flunitrazepam induces geometrical changes at the lipid-water interface. Colloids Surf B Biointerfaces 2001;20:63–72.
46. Garcia DA, Quiroga S, Perillo MA. Flunitrazepam partitioning into natural membranes increases surface curvature and alters cellular morphology. Chem Biol Interact 2000;129:263–277.
47. Pinto MA, Malheiros SVP, de Paula E, Perillo MA. Hydroxyzine, promethazine and thioridazine interaction with phospholipid monomolecular layers at the air-water interface. Biophys Chem 2006;119:247–255.
48. Lipowski R. Domains and rafts in membranes—hidden dimensions of self-organization. J Biol Phys 2002;28:195–210.
49. Rog T, Pasenkiewicz-Gierula M, Vattulainen I, Karttunen M. What happens if cholesterol is made smoother: importance of methyl substituents in cholesterol ring structure on phosphatidylcholine-sterol interaction. Biophys J 2007;92:3346–3357.